Wind Tunnel Measurements of Rolling Moment in a Swept-Wing Vortex Wake

Z. El-Ramly,* W.J. Rainbird,† and D.G. Earl‡
Carleton University, Ottawa, Canada

Some measurements of the trailing vortex system behind a 35° sweptback, tapered wing have been made in a low-speed tunnel at a chord Reynolds number of 0.5 x 10^6. Detailed wing loading was obtained from pressure distributions. Mean flow properties have been measured, using a non-nulling 5-hole probe, at two stations 2½ and 5 main wing spans downstream. Induced rolling moment on two trailing wings, which intercepted the main-wing vortex system, was also measured. Judged by the circulation around the core, the shear layers had not fully rolled up at the 2½*b* station. Also no further appreciable roll-up occurred at the 5*b* station. Furthermore, there was very little difference between the induced rolling moments measured at the two stations.

Introduction

In recent years, there has been renewed interest and activity (both theoretical and experimental) aimed at understanding the fluid mechanics of trailing vortices generated by aircraft (see for example Olsen, Goldberg and Rogers,[1] and El-Ramly[2] for surveys of the problem). The aim of all this work is, of course, to reduce the hazard resulting from light aircraft being upset by interaction with trailing vortices from heavily loaded large aircraft. If trailing vortex formation can be inhibited or if decay can be enhanced then flight time and distance spacings can be safely reduced.

Most of the wind-tunnel measurements of trailing vortices have been formed behind wings of rectangular planform.[3-10] At the time of planning for the present work the only set of measurements behind wings representative of current transport aircraft were those of Chigier and Corsiglia[7] in which hot-wire measurements were made behind a CV-990 model wing. However, the measurements were affected by vortex meander[9] which resulted from the high turbulence level in the working section of the wind tunnel used. Recently de Vries[11] conducted extensive loading and flow-field measurements on and behind an untapered 30° swept wing of aspect ratio 5, but only up to about one wing span downstream. Further results for swept wings, representative of the current generation of large transport aircraft, are clearly needed to fill the gap in experimental work.

Attempts to correlate different experimental results have usually not met with much success. The results of Grow[5] seem to suggest that the circulation and the maximum tangential velocity of the rolled up vortex are a function of wing aspect ratio and taper ratio, for unswept wings. In many experiments overall lift coefficient of the generating wing is used as the only basis for comparison yet in some ways it is inappropriate (from an inviscid flow point of view) since it artificially introduces the wing mean chord and disguises the fact that it is the nondimensional span loading intensity and distribution that is important in determining vortex roll-up and strength – see for example Refs. 12, 13, and 14 for vortex sheet roll-up calculations. It is clearly important in experiments that detailed wing loading be measured on the generating wing so as to render the results useful and make comparison with other measurements possible, especially if modifications to the wing or its tip are attempted.

Reduction in maximum tangential velocity or increase in core size have been used by some experimenters as a measure of reduced vortex hazard. However, the core usually represents only a small part of the flow field encountered by a following aircraft. The irrotational flow outside the core is not affected by the redistribution of streamwise vorticity within the core and since the wing of a following aircraft sees the whole flow field within its span a reduction of the velocity over a small fraction of the wing would not effectively reduce the maximum induced rolling moment. The present authors feel that a better and more direct measure of the effect of changing the core structure would be to measure the change of induced rolling moment impressed on a wing intercepting the vortex wake of the generating wing.

The present experimental study, conducted at model scale (approximately 1/50 full scale), is aimed at a general understanding of how the boundary layers from a representative sweptback wing roll-up, after separation, to form a concentrated vortex structure – the near-field problem. The particular aspect that is treated in this paper is the measurement of the induced rolling moment on two scaled wings that interact with the known concentrated vortex structure from the main wing at downstream distances of about 2½ and 5 spans.

Experimental Setup

The experiments have been carried out in the 20 x 30 in. low-speed return circuit wind tunnel at Carleton University at a test section speed of about 170 ft/sec. For the present program the test section, which is normally 6 ft long has been extended by adding an additional 16 ft of working section in place of the first diffuser of the wind tunnel. A schematic of the working section layout is shown in Fig. 1. The large half-wing (herein called the main wing), see Table 1, is sidewall mounted on an incidence gear and distributed suction is applied over an area of highly resistive sintered bronze material surrounding the root chord to avoid the unrepresentative end effects which could result from the interaction of the wing pressure field and the working section sidewall boundary layer. The main wing has 42 pressure plotting tubes let in to its upper and lower surfaces and pressure distributions can be taken at 14 spanwise stations using a clamping multitube manometer. The intercepting trailing wings, whose geometries (given in Table 1) were chosen to be representative of a light aircraft (Cessna 175) and a medium commercial transport (Boeing 737) respectively, were sting supported from a floor mounted traversing strut. The induced rolling moment on

Presented as Paper 75-844 at the AIAA 8th Fluid and Plasma Dynamics Conference, Hartford Conn., June 16-18, 1975; submitted June 27, 1976; revision received Feb. 27, 1976. This research was supported by the National Research Council of Canada, Grant A7799.

Index categories: Aircraft Testing (Including Component Wind-Tunnel Testing); Jets, Wakes, and Viscid-Inviscid Interactions.

*Research Associate. Member AIAA.

†Professor of Engineering. Member AIAA.

‡Research Assistant.

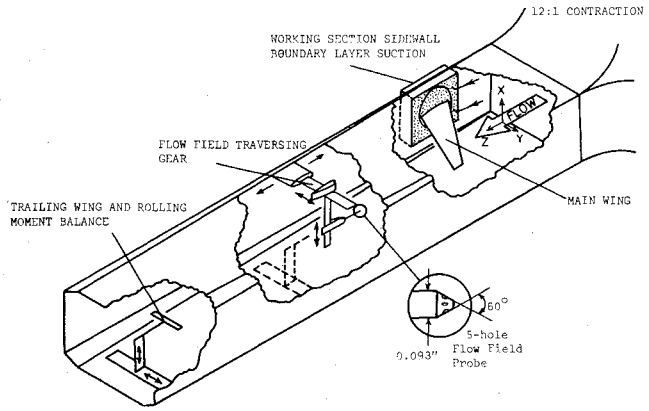

Fig. 1 Isometric sketch of working section.

Table 1 Wing dimensions[a]

	Main (Half wing)	Trailing wings	
		Straight wing	Sweptback wing
Span	21.0 in. (×2)	10.0 in.	20.0 in.
Relative span	1	0.24	0.48
Average chord	6.00 in.	1.33 in.	2.35 in.
Aspect ratio	7.0	7.5	8.5
Taper ratio	⅓	1	⅓
Sweepback (¼c)	35°	0°	35°
Wing twist	0°	0°	0°
Wing section	12%, symmetrical	NACA 64_2-015	NACA 64_2-015
Tip form	Half body	Square cut	Square cut

[a]Note: transition fixing on trailing wing with sand roughness strip (0.0057-0.0072 in.) to 15% chord on both surfaces.

these wings was measured on a simple strain-gauged cantilever element roll balance at the base of the sting and displayed versus lateral or vertical position on an x-y plotter. The wings were mounted horizontally (i.e. parallel to the main wing plane) at a nominal incidence of zero, at two downstream stations – about 2½ and 5 main wing spans downstream of the main wing mean ¼-chord position.

Flow-field measurements (local total pressure and three orthogonal mean velocity components) were made using a precalibrated nonnulling blunted conical 5-hole probe attached to a separate traversing mechanism which is mounted on continuous rails on the working section sidewall and which could be located at the same two downstream positions as were used for the trailing wing measurements. The individual pressures from the 5-hole probe were connected to pressure transducers and the outputs were plotted against lateral (or vertical) position as the probe was very slowly traversed through the vortex field. Basic nonuniformities of the flow field, probe misalignment, and upstream effects of the mechanism were accounted for by making separate traverse with the vortex-generating wing removed from its position near the upstream end of the extended working section. Similar precautions were taken with the rolling moment measurements.

The effect of the wind-tunnel walls on the roll-up process have been examined in a separte paper[14] and a more complete description of the experimental setup can be found in Ref. 15.

Discussion of Results

Some representative results will be presented and discussed. Figures 2 and 3 give the main-wing normalized loadings in the spanwise and chordwise directions at various angles of incidence up to and beyond the onset of tip and leading edge separation ('tip stall'). See also Table 2. Note that the angles of incidence have not been corrected for wind-tunnel wall constraint. These loadings have been obtained from the pressure distribution data. The spanwise loadings (Fig. 2), for overall C_L's up to about 0.6, form a single curve (there is no wing twist) and when compared with elliptic loading indicate (as expected) higher loading near the wing tip. At higher incidence progressive 'tip stall' resulting from flow separation, first along the streamwise tip and then along the outboard part of the leading edge, unloads the outboard sections between about 0.6 and 0.9 of the semispan and transfers the load to the root.

The chordwise loading (Fig. 3) is 'flat-plate-like' (the wing sections are symmetrical) from about 0.35 to 0.85 of the semispan. Due to the Low Reynolds number of the tests $R_c = 0.5 \times 10^6$, viscous effects are quite strong and reduce the chordwise loading to very low values near the trailing edge $x/c > 0.8$. The center 'kink-effect,' a characteristic of sweptback wings, results in flattened loadings near the root, extending out about one root chord length, that is to about 40% semispan. Similarly, the 'tip-effect,' associated with the unloading effect of the wing tip, extends inboard about one tip chord (about 15% semispan) giving more peaky loadings, at least prior to tip stall.

The overall lift characteristics of the main and trailing wings are given in Fig. 4. For the main wing the lift coefficient has been obtained from a double integration of the pressure distributions whereas the lift characteristics of the trailing wings were directly measured on a 3-component overhead external balance. Again no angle of incidence corrections have been applied to the data presented. To avoid irregular behavior due to laminar separations, because of the low test Reynolds numbers, transition was fixed on the trailing wings using sand roughness strips (see Table 1). Even with this precaution low maximum lift coefficients were obtained.

Table 2 Local lift coefficient and normalized spanwise loading

Station no.		1	2	3	4	5	6	7	8	9	10	11	12	13	14
	$2y/b$	0.071	0.143	0.214	0.286	0.357	0.429	0.476	0.571	0.643	0.714	0.786	0.857	0.929	0.988
$\alpha = 5°$,	C_L	0.305	0.316	0.329	0.329	0.337	0.345	0.363	0.372	0.383	0.386	0.388	0.375	0.333	0.208
$\bar{C}_L = 0.341$	$\frac{cC_L}{\bar{c}\bar{C}_L}$	1.277	1.258	1.240	1.174	1.132	1.086	1.092	1.015	0.963	0.890	0.814	0.708	0.558	0.312
$\alpha = 11°$,	C_L	0.696	0.719	0.749	0.747	0.762	0.773	0.771	0.767	0.765	0.750	0.754	0.732	0.655	0.451
$\bar{C}_L = 0.734$	$\frac{cC_L}{\bar{c}\bar{C}_L}$	1.354	1.329	1.312	1.237	1.187	1.128	1.075	0.970	0.893	0.803	0.733	0.641	0.510	0.315

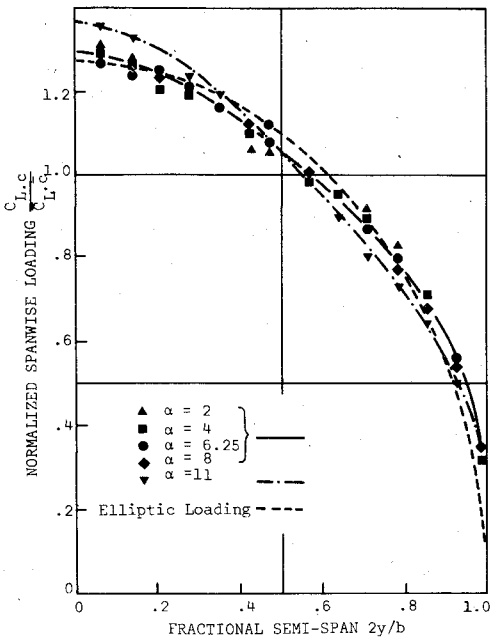

Fig. 2 Spanwise loading on main wing.

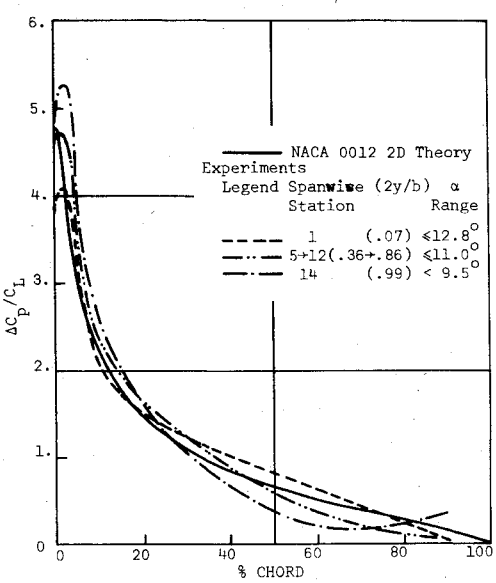

Fig. 3 Normalized chordwise loading on main wing.

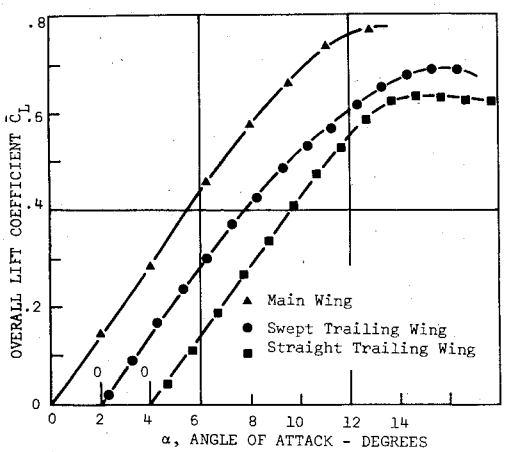

Fig. 4 Lifting characteristics of main and trailing wings.

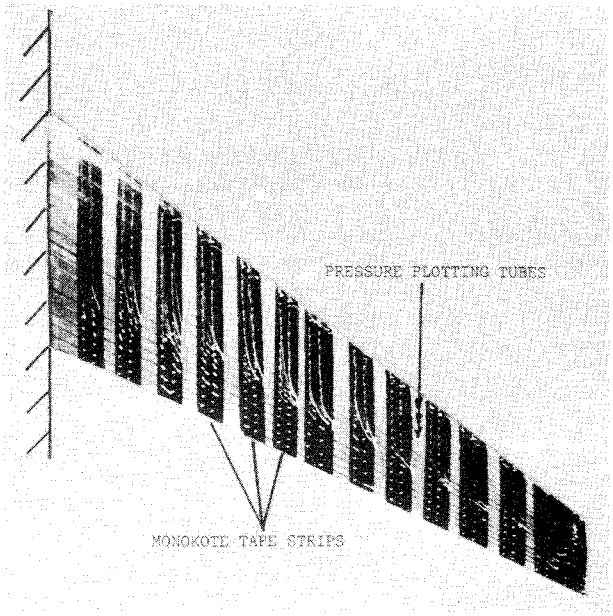

Fig. 5 Upper-surface flow vizualization, $\bar{C}_L = 0.74$.

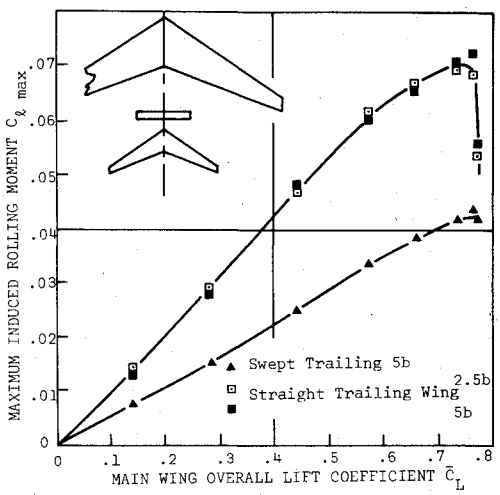

Fig. 6 Maximum induced rolling moment on trailing wings vs main wing overall lift coefficient.

On the main wing oil dot flow vizualization, as shown for a typical case in Fig. 5, revealed that a short laminar separation bubble, due to the large leading radius of the section used, was present giving turbulent boundary-layer conditions downstream of reattachment. This turbulent state of the main-wing boundary layers was confirmed by limited hot-wire measurements. Flow vizualization photographs and detailed pressure distributions show that a progressive 'tip stall' developed beyond an incidence angle of about 8°, $\bar{C}_L = 0.6$, but a serious decrease in overall lift curve slope is not evident until $\alpha = 11°$, $\bar{C}_L = 0.74$. By the time this lift coefficient (0.74) is achieved the surface shear stress near the trailing edge on the wing upper surface is quite low in magnitude (short oil dot traces) and is directed essentially parallel to the trailing edge – see Fig. 5.

Typical rolling moment results measured on the trailing wings at two downstream locations (2½ and 5 main wing spans) are shown on Figs. 6 and 7. The maximum rolling moment coefficient,

$$C_{\ell_{max}} = \frac{R.M._{max}}{\frac{1}{2}\rho V_\infty^2 Sb}$$

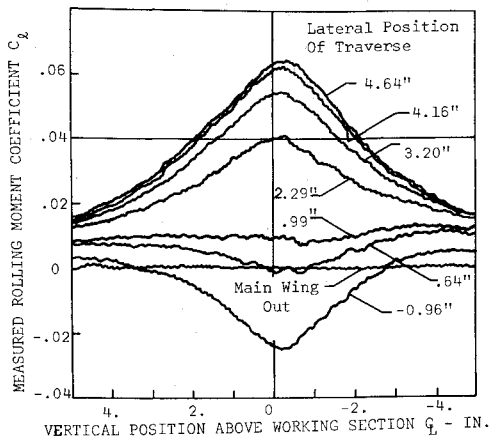

Fig. 7 Variation of induced rolling moment coefficient on straight trailing wing, $\overline{C_L} = 0.74$.

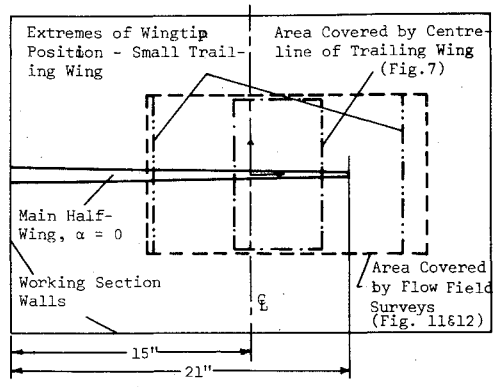

Fig. 8 Sketch showing measurement regions in the cross-flow plane (looking upstream).

where S and b are the appropriate wing area and span, increases with overall wing $\overline{C_L}$ up to about $\alpha = 11°$, $\overline{C_L} = 0.74$, and exhibits a slight nonlinearity (due to a somewhat more complete roll-up at higher $\overline{C_L}$'s). However once tip stall becomes dominant, and the vortex structure more dispersed, the rolling moment induced on the smaller wing falls rapidly for $\overline{C_L} > 0.75$. The swept trailing wing does not experience such a rapid fall-off of rolling moment, because of its larger span and the relatively smaller fraction of the span that is affected by the vortex dispersion compared to the outer 'inviscid' part of the flow. No significant attenuation in maximum induced rolling moment is observed between the two downstream measuring stations, even though the distance from the main wing has doubled.

Variation of rolling moment coefficient on the small straight wing with vertical position in the working section for various lateral stations is shown in Fig. 7 – copied directly from the x-y recorder output. (The position of these and the subsequent flow-field traverses is shown on Fig. 8). As indicated in the preceding a main-wing-out traverse is also run to remove irregularities of the undisturbed airstream and model wing manufacturing errors. From results such as those displayed in Fig. 7, it is possible to construct Fig. 6.

Figures 9 and 10 give a comparison of the measured and calculated rolling moment coefficient on the small straight wing at the $2\frac{1}{2}b$ and $5b$ downstream stations at main wing $\overline{C_L}$'s of 0.34 and 0.74. A theoretical calculation using the simple model of a single infinite line vortex of strength equal to the measured circulation around a circuit near the 'core' (just outside the viscous region), coupled with a strip theory calculation across the wing span, gives very reasonable agreement for a main wing $\overline{C_L}$ of 0.34. However the same method somewhat overestimated the induced rolling moment

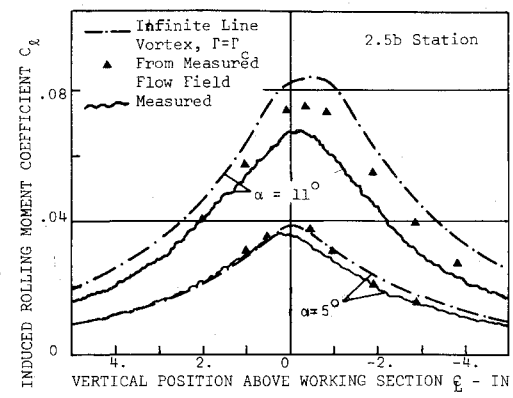

Fig. 9 Variation of induced rolling moment on straight wing (vertical scan at lateral position of maximum induced roll). $2\frac{1}{2}b$ Station.

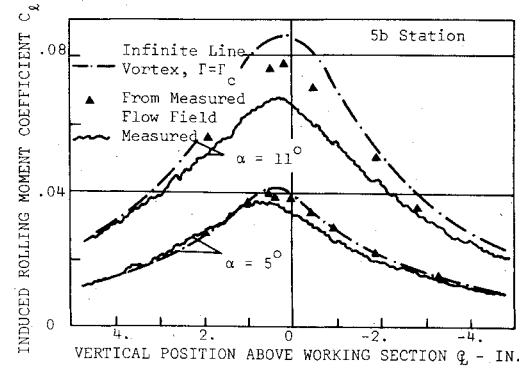

Fig. 10 Variation of induced rolling moment on straight wing (vertical scan at lateral position of maximum induced roll). $5b$ Station.

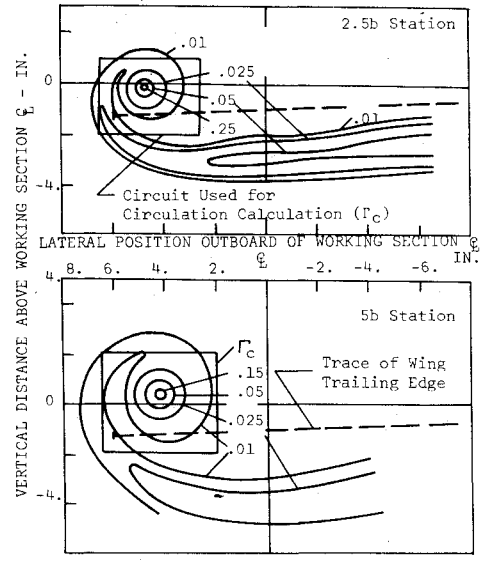

Fig. 11 Contours of equal total pressure loss coefficient $(P_{o_\infty} - P_o)/\frac{1}{2}\rho V_\infty^2$ for $\alpha = 5°$, $C_L = 0.34$.

coefficient values for main wing $\overline{C_L}$ of 0.74, especially near the maximum roll. The flattening of this theoretical curve (for $\overline{C_L} = 0.74$) mear maximum rolling is due to the high induced flow angles and the imposed limiting maximum lift characteristic of the straight trailing wing (see Fig. 4).

More reasonable estimates for the calculated rolling moment are obtained using the measured flow field (see the following) as an input to the still comparatively crude strip theory calculation on the trailing wing. The difference between the calculations using a line vortex model compared to the measured flow field, is largely because the vortex core is

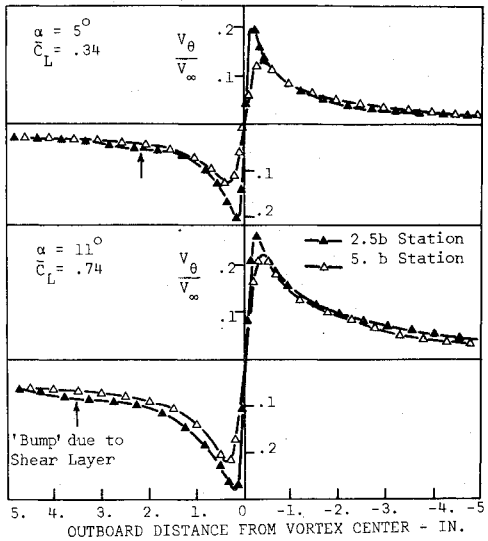

Fig. 12 Normalized tangential velocity (lateral scans through vortex center).

not represented in the former and the flow field is not, of course, axisymmetric. The difference between the measured rolling moment coefficient and that calculated using the measured flow field is due to the combined effect of using a simple strip theory and assuming that the local sectional lift slope is the same as the overall lift slope together with limiting the maximum lift. No refinement to the theoretical calculation scheme is intended at this time because the whole idea behind the present investigation is to examine the feasibility of using a trailing wing to assess, in an overall way, a vortex flow field and to simply study the effects of any modification to it, from the point of view of a trailing aircraft.

Some sample flow-field results are displayed in Figs. 11 and 12 – more complete results are given in Ref. 15. Figure 11 shows the contours of total pressure loss coefficient at the $2\frac{1}{2}b$ and $5b$ stations for a main wing $\overline{C_L}$ of 0.34 (the results for $\overline{C_L}$ of 0.74 are much the same but with a more diffuse core and shear layer). It is clear from Fig. 11 that the vortex is not fully rolled up; even at the $5b$ downstream station, a considerable remnant of the original wake being visible. Furthermore, by calculating the circulation around a circuit,[§] see Fig. 11, near the 'core' close to the boundary of the viscous region (defined arbitrarily by the 1% total pressure loss line) it was found that for $\overline{C_L}$ of 0.34 only 41% of the circulation derived from the corresponding wing spanwise loading is concentrated around the core at the $2\frac{1}{2}b$ station while at the $5b$ station it is 43%. The corresponding figures for $\overline{C_L}$ of 0.74 are 48% at the $2\frac{1}{2}b$ station and 51% at the $5b$ station. The conclusion then is that there is very little further roll-up between the $2\frac{1}{2}b$ and $5b$ downstream stations, and that the shear layers, resulting from the separation of the boundary layers on the main wing, are already effectively fully rolled up at the $2\frac{1}{2}b$ station; but not in the traditional sense of being axisymmetrical vortices.

From the tangential velocity distributions on Fig. 12 and defining as the core center the point of zero cross-flow velocity, then one might conclude based on this evidence that we have a fully rolled up axisymmetric vortex (particularly if the minor bump in the curve due to crossing the discrete shear layer is ignored). However this is not a correct conclusion as the total pressure loss contours (Fig. 11) show. Figure 12 also shows that the maximum tangential velocity, for a main wing $\overline{C_L}$ of 0.34 drops from about 0.20 to 0.12 V_∞, with a corresponding increase in core size, between the $2\frac{1}{2}b$ station and $5b$ station. Somewhat similar behavior is evident at the higher lift coefficient (0.74) although the relative drop in tangential velocity (from about 0.28 to 0.22) is less. However, as noted previously, the measured maximum induced rolling moment on the trailing wings does not show any corresponding attenuation between the two stations. Maximum tangential velocity reduction or core size expansion cannot then be used as sole measures of decreased vortex hazard unless supported with other evidence that the modified configuration is more unstable and that this will enhance vortex dissipation and decay.

§The circuits chosen must of course enclose all the streamwise vorticity near the core i.e. must embrace the rolled up part of the shear layers from the wing. Larger circuits which still exclude the remnant shear layer, would not enclose any more vorticity but would decrease the accuracy with which Γ_c can be determined due to the smaller cross-flow velocity components that exist further from the core.

Conclusions

Wind-tunnel measurements of the trailing vortex system behind a 35° sweptback wing have been made at moderate lift coefficients, 0.34 and 0.74, and at a mean chord Reynolds number of about 0.5 x 10^6. The measurements include wing loading and detailed flow field measurements, as well as induced rolling moments on two trailing wings.

Up to 5 wing spans (35 mean chords) downstream of the generating wing it was found that the shear layers separating from the wing have not yet fully rolled up since only about 45% of the wing root circulation appears around the vortex core. Moreover, judging by the circulation measured around the vortex 'core' (the rolled up part of the shear layers) very little further roll-up occurred between the $2\frac{1}{2}$ and 5 span measuring stations. This suggested that, for the present test Reynolds number, the shear layers are already effectively fully rolled up at the $2\frac{1}{2}$ span station even though not in an axisymmetric form.

The induced rolling moment on trailing wings, which confirm the aforementioned conclusions on the flow field, has proved to be a valuable tool in trailing vortex measurements. Not only do such measurements give a practical assessment of the resulting vortex hazard and of gross changes in core structure, but also they give an easy single measurement that can indicate the degree of shear-layer roll-up.

Until the complete fluid dynamics of the trailing vortex problem are much better understood, it is recommended that, when doing experimental work in ground based facilities, the detailed loading and boundary-layer characteristics on the generating wing be included in the measurements.

References

[1] Olsen, J., Goldberg, A., and Rogers, M., *Aircraft Wake Turbulence and Its Detection*, Plenum Press, New York, 1971.

[2] El-Ramly, Z., "Aircraft Trailing Vortices: A Survey of the Problem," Carleton University, Ottawa, Canada, ME/A 72-1, Nov. 1972.

[3] Dosanjh, D.S., Gasparek, E.P., and Eskinazi, S., "Decay of a Viscous Trailing Vortex," *Aeronautical Quarterly*, Vol. 13, May 1962, pp. 167-188.

[4] McCormick, B.W., Tangler, J.L., and Sherrieb, H.E., "Structure of Trailing Vortices," *Journal of Aircraft*, Vol. 5, May-June 1968, pp. 260-267.

[5] Grow, T.L., "Effect of Wing on Its Tip Vortex," *Journal of Aircraft*, Vol. 6, Jan-Feb. 1969, pp. 37-41.

[6] Logan, A.H., "Vortex Velocity Distributions at Large Downstream Distances," *Journal of Aircraft*, Vol. 8, Nov. 1971, pp. 930-932.

[7] Chigier, N.A. and Corsiglia, V.R., "Wind Tunnel Studies of Wing Wake Turbulence," AIAA Paper 72-41. San Diego, Calif., Jan. 1972.

[8] Mason, W.H. and Marchman, J.F., "The Farfield Structure of Aircraft Wake Turbulence," AIAA Paper 72-40, San Diego, Calif., Jan. 1972.

[9] Corsiglia, V.R., Schwind, R.G., and Chigier, N.A., "Rapid Scanning, Three Dimensional Hot-Wire Anemometer Surveys of Wing-Tip Vortices," *Journal of Aircraft*, Vol. 10, Dec. 1973, pp. 752-757.

[10] Orloff, K.L., "Trailing Vortex Wind Tunnel Diagnostics with a Laser Velocimeter" *Journal of Aircraft,* Vol. 11, Aug. 1974, pp. 477-482.

[11] de Vries, O., "Wind Tunnel Investigation of the Development of the Vortex Wake Behind a Sweptback Wing," National Aerospace Laboratory, The Netherlands, NLR-TR-72017U, Mar. 1973.

[12] Donaldson, C. duP., "A Brief Review of the Aircraft Trailing Vortex Problem," AFOSR-TR-71-1910, A.R.A.P. Rpt. No. 155, May 1971.

[13] Spreiter, J.R. and Sacks, A.H., "The Rolling Up of the Trailing Vortex Sheet and Its Effect on the Downwash Behind Wings," *Journal of the Aeronautical Sciences,* Vol. 18, Jan. 1951, pp. 21-32.

[14] Mokry, M. and Rainbird, W.J., "Calculation of Vortex Sheet Roll-up in a Rectangular Wind Tunnel," *Journal of Aircraft,* Vol. 12, Sept. 1975, pp. 750-752.

[15] El-Ramly, Z. "Investigation of the Development of the Trailing Vortex System Behind a Swept-Back Wing," Carleton University, Ottawa, Canada, ME/A 75-3, Oct. 1975.